DRAFT VERSION OCTOBER 9, 2003
Preprint typeset using LaTeX style emulateapj v. 7/15/03

COULD THERE BE A HOLE IN TYPE IA SUPERNOVA?

DANIEL KASEN, PETER NUGENT, ROLLIN THOMAS & LIFAN WANG
Lawrence Berkeley National Laboratory, M.S. 50-F, 1 Cyclotron Road, Berkeley, CA 94720

(Received; Accepted)
Draft version October 9, 2003

ABSTRACT

In the favored progenitor scenario, Type Ia supernova result from a white dwarf accreting material from a nearby, non-degenerate companion star. Soon after the white dwarf explodes, the ejected supernova material will run over the companion star, and in the interaction a substantial asymmetry can be imprinted on the supernova ejecta. Two-dimensional hydrodynamical simulations by Marietta et al. (2000) show that the companion star carves out a conical hole of opening angle 30°-40° in the supernova ejecta. In this paper we preform multi-dimensional Monte Carlo radiative transfer calculations to explore the observable consequences of an ejecta-hole asymmetry. We find that the aspherical supernova looks normal for almost all lines of sight *except* when one looks almost directly down the hole. In the later case one sees a brighter supernova with a peculiar spectrum characterized weaker absorption features, and lower absorption velocities, and features from the deeper, more ionized material. The spectra which emanate from the hole are comparable to the class of SN 1991T-like supernova. We consider how the ejecta-hole asymmetry may explain the current spectropolarimetric observations of SN Ia, and suggest a few polarization signatures of the geometry. Finally, we discuss the variations currently seen in observed SN Ia and how an ejecta-hole asymmetry may fit in as one of several possible sources of diversity.

Subject headings:

1. INTRODUCTION

1.1. *Asymmetry of Type Ia Supernova*

Some Type Ia supernova (SN Ia) are known to be aspherical; direct evidence for this comes from optical spectropolarimetric observations. For a spherically symmetric system, the polarization integrated over the projected supernova surface cancels – a non-zero polarization detection demands some degree of asymmetry. The measured intrinsic polarization of SNe Ia is relatively small, but certainly detected in a few cases: SN 2001el, a normal SN Ia, was polarized at about 0.4% (Wang et al. 2003); the underluminous and spectroscopically peculiar SN 1999by at about 0.7% (Howell et al. 2001).

The asphericity of SNe Ia is closely tied to the supernova explosion physics and progenitor system, both of which are still under debate. But little is known about the shape of the ejecta. Unfortunately, all observed SN Ia are too distant to be resolved, and it is hard to reconstruct the ejecta's detailed three-dimensional geometry from polarization measurements, as this constitutes a kind of ill-posed inverse problem. In both SN 1998by and SN 2001el the polarization angle was roughly constant across the majority of line features, which tells us that the bulk of the ejecta obeyed a near axial symmetry. Most theoretical attempts at modeling the spectropolarimetry have so far assumed the ejecta was ellipsoidal (Howell et al. 2001; Jeffrey 1991). A shape like that might arise, for example, in the explosion of a rapidly rotating progenitor star.

Another potential cause of asymmetry in SN Ia is the binary nature of the progenitor system. In the favored progenitor scenario (the *single-degenerate scenario*; see Branch et al. (1995) and references therein), SNe Ia result from a white dwarf accreting material from a non-degenerate companion star. The companion may be either a main sequence star, a red-giant, or a subgiant; as it is close enough to be in Roche-lobe overflow, it subtends a substantial solid angle from the perspective of the white dwarf. The supernova explosion occurs when the white dwarf has accreted enough matter that the densities and temperatures at the center are sufficient to ignite Carbon, just below the Chandrasekhar limit. The ejected supernova material moves at a few percent of the speed of light and soon after the explosion (from minutes to hours) will run over the companion star. In the impact it would not be surprising if a substantial asymmetry was imprinted on the supernova ejecta.

The ejecta-companion interaction has been studied with two-dimensional hydrodynamical models by Fryxell & Arnett (1981); Livne et al. (1992), and most recently and extensively by Marietta et al. (2000). These studies were primarily concerned with the fate of the companion star, in particular how much hydrogen gets stripped from its outer envelope. Stripped hydrogen may appear as narrow Balmer emission lines in the supernova spectrum, which if observed would provide direct evidence of a binary progenitor system. Observers searched many years for Hydrogen in SNe Ia, but no trace was found until just recently, for SN 2002ic(Hamuy et al. 2003). The observations of SN 2002ic, however, suggest that the supernova ejecta was interacting with a Hydrogen-rich circumstellar environment, rather then indicating stripped companion material.

With the advance of spectropolarimetric observations, the nature of SN Ia asphericity becomes another relevant test of the single-degenerate progenitor scenario. In their hydrodynamical models, Marietta et al. (2000) find that the impact with the companion star carves out a conical hole in the supernova ejecta. The opening angle

Electronic address: e-mail:dnkasen@panisse.LBL.gov

of the hole is 30°-40°, and because the ejecta is moving supersonically the hole does not close with time. The final configuration is axially symmetric, as was seen in the polarization observations of SN 2001el.

In this paper we use three-dimensional (3-D) radiative transfer calculations to address the possibility of SNe Ia having an ejecta hole asymmetry. We calculate the line of sight variations of the spectrum, luminosity, and polarization for the aspherical supernova near maximum light. In contrast to the ellipsoidal models, the line of sight variations in an ejecta-hole geometry can be rather extreme, especially when one looks near the hole itself. These variations would necessarily introduce some diversity into the observed properties of SNe Ia. Therefore we ask: exactly what type of diversity arises in the ejecta-hole geometry and does this fit in in with the diversity already known to exist in SN Ia?

While SN Ia are considered to be a rather homogeneous class of objects, they do show some variety in their spectral and photometric properties. The observed peak magnitudes of SN Ia, for instance, vary by ~ 0.3 mag, and the brightness is found to correlate with the width of the light curve (Phillips et al. 1999). The spectra of SNe Ia can be classified as either normal or peculiar (Branch et al. 1993). The peculiar spectra have feature strengths that differ from "normal" cases (such as SN 1981B), and are subdivided into two classes: SN 1991bg-like peculiars have a broad Ti II absorption trough not seen in the normals (Filippenko et al. 1992a). SN 1991T-like supernova have weak or absent features from singly ionized species but noticeable Fe III lines (Filippenko et al. 1992b; Phillips et al. 1992; Jeffery et al. 1992). Not all supernova fit cleanly into the classification scheme. In its premaximum spectra, SN 1999aa closely resembled SN 1991T, but by maximum light it had it began to look much more normal, with Si II and Ca II lines that were stronger than SN 1991T although weaker than normal (Li et al. 2001b). As such SN 1999aa is considered by some to be an intermediate link between the normal and the SN 1991T-like supernova. Other observations have uncovered singular objects like SN 2000cx (Li et al. 2001a) and SN 2002cx (Li et al. 2003), that while resembling SN 1991T in some ways (weak Si II, strong Fe III lines) showed other peculiarities that were unique. Additional spectral diversities include the abnormally high photospheric velocities of SN 1984A(Branch 1987) and detached high velocity features seen in several supernova (Hatano et al. 1999; Wang et al. 2003; Thomas et al. 2003). The diversity of SNe Ia is thus multi-faceted, a point we return to in the conclusion.

2. THE EJECTA-HOLE MODEL

2.1. *Density and Composition Structure*

The ejecta model used in the calculations is based on the spherical w7 explosion model (Nomoto et al. 1984), which has often been used to modeling the spectra of normal SN Ia in spherical radiative transfer calculations (Lentz et al. 2001; Jeffery et al. 1992; Nugent et al. 1997). The composition structure of w7 consists of an inner ^{56}Ni zone ($v < 9000$ km s^{-1}), a middle zone of intermediate mass elements (9000 km s$^{-1} < v <$ 15,000 km s^{-1}) and an outer unburned region of Carbon-Oxygen rich material ($v > 15,000$ km s^{-1}). In our calculations we found it necessary to make one adjustment to the compositions. To reproduce the depth and width of the Ca II H&K feature in a normal SN Ia, we need to increase the Calcium abundance by a factor of 10 in the outer C-O region. The difficulty w7 has in fitting the Ca II H&K feature has already been noted by Lentz et al. (2001) in the context of detailed NLTE models. The lack of burned material above 15,000 km s^{-1}in w7 may indicate a weakness of the parameterized deflagration explosion mechanism used.

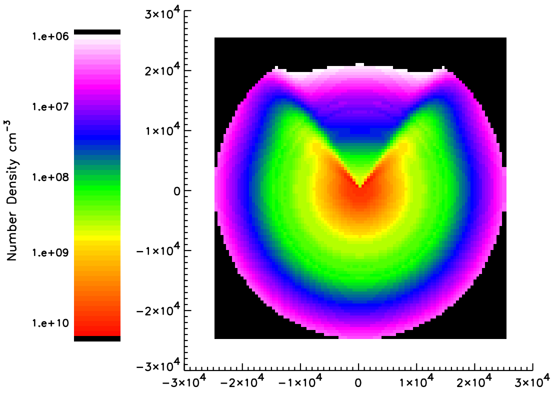

FIG. 1.— Density structure of the ejecta-hole model near maximum light (20 days after explosion).

To introduce an ejecta hole into the spherical model, we describe the density structure by an analytic function that in the radial direction well approximates w7:

$$\rho(v, \theta) = \rho_0 \exp(-v/v_e) F(\theta) \quad (1)$$

where $v_e = 2,500$ km s^{-1}and ρ_0 is set by the condition that total mass of the ejecta equals a Chandrasekhar mass. $F(\theta)$ is an angular density variation function which would equal one in a spherical model. For the ejecta-hole model, we use a constructed function which resembles the structure seen in the interaction models of Marietta et al. (2000). The conical hole has a half opening angle of $\theta_H = 40°$ and the density in the hole is a factor $f = 0.05$ less then that outside. The material that is displaced from the hole gets piled up into a density peak just outside the hole edge, with angular size $\theta_P = 20°$. The function invented to reproduce these features is:

$$F(\theta) = f_H + (1 - f_H)\left(\frac{x^n}{1 + x^n}\right)\left(1 + Ae^{-(\frac{\mu-\mu_H}{\mu_P})^2}\right) \quad (2)$$

where

$$x = \frac{1 - \mu}{\mu_H} \quad (3)$$

and $\mu = \cos\theta$ and $n = 8$. The constant A is set by the condition that the mass within a shell is equal to that in the spherical model (i.e the integral of $F(\theta)$ over solid angle is equal to 4π). The density structure is shown in Figure 1.

This analytic function does not capture all the complexity present in a hydrodynamical model; for example, Marietta et al. (2000) point out that the opening angle of the hole is smaller at high velocities than low velocities

($\sim 30° - 35°$ as opposed to 40°). Of course, the benefit of using a simple analytic function is that it isolates the essential geometrical consequences of a hole asymmetry. In addition it allows us to test how varying the eject hole structure affects the observable signatures. Once the general ideas are understood, one can perform more detailed calculations based on hydrodynamical models using a wide range of initial conditions.

In the ejecta/companion interaction as much as 0.1-0.5 $M_\odot$ of hydrogen rich material can be stripped and ejected from the companion star Wheeler et al. (1975); Marietta et al. (2000). This material is not included in our calculations. The vast majority of the stripped material has low velocity ($v < 1000$ km s^{-1}) and sits at the center of the ejecta, where it will not affect the spectrum or polarization near maximum light. A small amount of material may be ejected at high velocities and could be related to the high-velocity spectral features seen in SN 2001el (Wang et al. 2003) and SN 2000cx (Li et al. 2001a). Branch et al. (2003) Thomas et al. (2003) have suggested an identification of high-velocity H_β in SN 2000cx, which if correct would suggest that the material was associated with a companion in some way. While not addressed in this paper, the observable consequences of the stripped material should be explored further with 3-D transfer calculations that include a NLTE treatment of hydrogen.

2.2. *Monte Carlo Code*

Our calculations are done using a Monte-Carlo (MC) radiative transfer code, described in detail in (Kasen 2003). The code applies MC principles laid out in, for example, Lucy (1999); Mazzali & Lucy (1993); Code & Whitney (1995). Although the code can handle arbitrary 3-D configurations, for the axially-symmetric models of this paper we use a 2-D Cartesian grid of 10^4 cells. In the MC approach, photon packets are emitted from within the supernova envelope and tracked through randomized scatterings and absorptions until they escape the atmosphere. Each packet contains a Stokes vector which describes its polarization state. All packets escaping in a certain direction are collected to construct the spectrum and polarization of the supernova along that line of sight. Our calculations use 100 angular bins, equally spaced in $\cos\theta$, to collect escaping photon packets.

One important issue in multidimensional MC transfer is where to place the initial source of photon packets. Most MC calculations emit packets from a spherical inner boundary surface (the 'light bulb"). In an ejecta-hole model, however, the hole would expose the inner boundary surface and provide a poor representation of the geometry. Therefore we perform a 2-D gamma ray transfer calculation to determine where radioactive energy from decaying ^{56}Ni and ^{56}Co is deposited in the supernova envelope (see § 3.1). The optical photon packets are then emitted from individual cells throughout the atmosphere, proportional to the local instantaneous energy deposition rate. There is no inner boundary surface, and photons are allowed to propagate throughout the entire supernova envelope, including the optically thick center. Overall, this approach is likely a good approximation to the actual conditions in SN Ia, as the luminosity at maximum light is dominated by radioactive energy deposition. However a proper treatment would also take into account diffusive energy stored in the supernova envelope by solving the full time-dependent radiative-hydrodynamics problem.

The opacities used in the calculation are electron scattering and bound-bound transitions; we ignore bound-free and free-free opacities as these are much less important in SN Ia atmospheres (Pinto & Eastman 2000b). Excitation and ionization are computed assuming LTE, where the temperature structure of the atmosphere is determined self-consistently using an iterative approach which imposes radiative-equilibrium. Line processes included are absorption and scattering, according to a two level atom with thermalization parameter $\epsilon = 0.05$, (Nugent et al. 1997). Because the detailed NLTE source function of the material is not calculated, packets are initially emitted according to a blackbody distribution with characteristic temperature T_{bb}. We choose T_{bb} so as to reproduce the continuum in the red end of the observed spectrum. The blue end of the spectrum shows very little dependence on T_{bb}, as packets with $\lambda \lesssim 6000\mathring{A}$ are absorbed and re-emitted in lines. The photon packets are initially emitted unpolarized but acquire polarization by electron scattering. Line scattered light is assumed to be unpolarized due to complete redistribution, as in the models of Howell et al. (2001), Höflich et al. (1996) and Kasen et al. (2003).

3. RESULTS

We have computed the gamma-ray deposition, optical spectrum, luminosity and polarization of the ejecta hole model near maximum light (20 days after the explosion). In this model the total luminosity is $L = 1.4 \times 10^{43}$ ergs and the emission temperature $T_{bb} = 11,000$ K. We discuss the various results in turn.

3.1. *Gamma Ray Deposition*

In the w7 explosion models, 0.6 $M_\odot$ of radioactive ^{56}Ni is synthesized. The decay of ^{56}Ni and its daughter ^{56}Co powers the supernova luminosity. 95% of the decay energy is in the form of gamma rays and 5% in positrons. The positrons are assumed to deposit their energy locally. We compute the gamma ray deposition with a Monte-Carlo transfer code that includes Compton and photo-electric opacity and also produces gamma ray spectra. The dominant opacity is Compton – after just a few Compton scatterings, a gamma ray has given up the majority of its energy.

In a spherical SN Ia model, the gamma ray trapping is very effective at maximum light. In the inner ^{56}Ni zone, the mean free path to Compton scattering is only 300 km s^{-1}and so the gamma rays deposit their energy nearly coincident to where they are created; only about 4% of the gamma ray energy escapes the atmosphere. Inside an ejecta hole, on the other hand, the mean free path is 20 times greater due to the lower density. Gamma rays generated in the hole can therefore escape the atmosphere, at least those that are emitted in the outward direction. This isn't that great a loss, however, as the mass of ^{56}Ni in the hole is less then 1% of the total. There is more ^{56}Ni ($\sim$11% of the total) in the material that has been displaced from the hole and is piled up around the edge. The density is high in the pile up and the gamma ray trapping is even more efficient than in a spherical model. Thus we find the perhaps unexpected result that the ejecta hole actually slightly enhances the

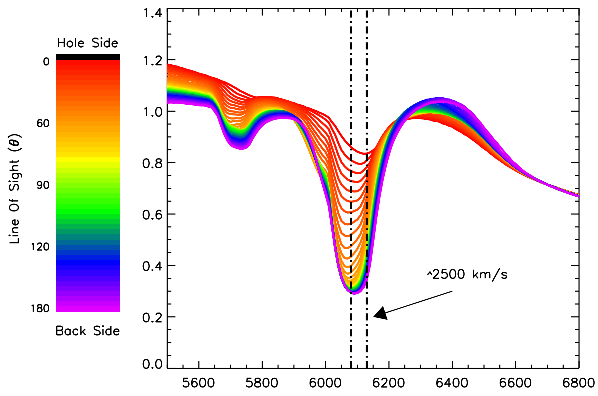

FIG. 2.— Flux profile of the Si II 6150 line (at maximum light) from various lines of sight. When viewed down the hole ($\theta = 0°$) the absorption trough is weaker and has a lower velocity by $\sim 2,500$ km s^{-1}.

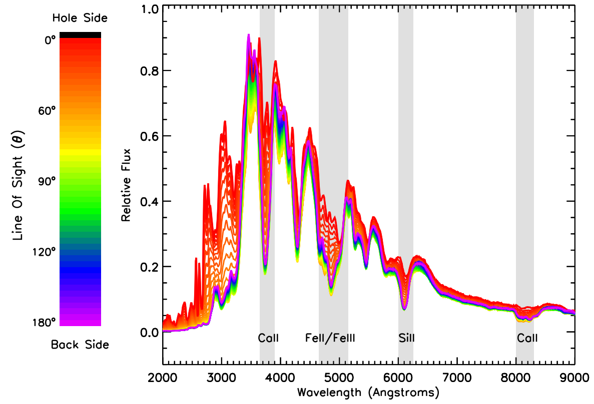

FIG. 3.— Spectrum of the ejecta-hole model near maximum light from various lines of sight. Some important line features are highlighted.

gamma ray trapping at maximum light, from 96% to 97%.

3.2. *Spectral Signatures*

3.2.1. *The P-Cygni Profile*

Line opacity in a spherical, expanding SN atmosphere gives rise to the well known P-Cygni profile – i.e. a blueshifted absorption trough with a redshifted emission peak. An ejecta-hole asymmetry dramatically alters the line profile from some lines of sight, as shown in Figure 2. The major effects are easily understood: in the typical P-Cygni formation, material in front of the photosphere occults the light below and gives rise to the blueshifted absorption feature. When one looks down the ejecta hole ($\theta < \theta_H$), the density of this occulting material is much lower and thus so are the line optical depths; the line absorption features are therefore much weaker. There is little change, however, in the redshifted emission component. Thomas et al. (2002) have pointed out that asymmetries have the most dramatic effect on absorption features, as the absorption depth is related directly to how much of the photosphere is covered by line opacity.

In addition, the minimum of the absorption features are generally less blueshifted when viewed down the hole, which can be understood as seeing deeper into the supernova ejecta. In fact the hole uncovers inner layers of ejecta which would otherwise be buried underneath the photosphere. Recall that in spherical models, the P-Cygni features are caused primarily by material above the photosphere – below the photosphere multiple electron scattering tends to wash out the line formation by establishing a near isotropic radiation field. However in the low density ejecta hole, the electron scattering photosphere is effectively removed – radiation streams radially out of the hole and absorption features form material at depth. This material will tend to be hotter, more ionized and perhaps of a different composition then the material above the photosphere. In our models, the minima of the absorption features typically form about 3000 km s^{-1}deeper when viewed down the hole as compared to a spherical model. Material much deeper in the ejecta (i.e. nearer the tip of the conical hole) corresponds to only a small fraction of the projected surface area of the supernova, and does not obscure enough light to produce noticeable absorptions.

As one looks away from the hole, the absorption depth increases rapidly, until for $\theta > \theta_H$ the depth is equal to that of the spherical model. For side-on views ($\theta \approx 90°$), the hole is in the emission region – because some emitting material is then lacking one expects the P-Cygni emission feature to be depressed near the line wavelength center. The missing material, however, amounts to only 11% of the total emitting area, so the effect is hardly noticeable. For $\theta > \theta_H$, the line profile changes very little with inclination.

3.2.2. *Spectrum Near Maximum Light*

In sum, the spectrum in the ejecta-hole model will look the same as in a spherical model for all lines of sight *except* when one looks almost directly down the hole ($\theta < \theta_H$). In the later case one sees a peculiar spectrum characterized by more highly ionized species, weaker absorption features, and lower absorption velocities. We show the line of sight variation of the maximum light spectrum in Figure 3. Notice in particular the dramatic effect the hole has on the Si II feature near 6150 Å, the Ca II H&K feature, and the iron blend near 5000 Å.

Figure 4 compares the model spectra to two well known SN Ia. The view away from the hole ($\theta = 90°$) resembles the normal Type Ia SN 1981B. The model reproduces most of the major features, except for a few discrepancies. The most obvious is that the flux peak near 3500 Å is much to large in the model. The opacity at this wavelength is largely due to Co II lines; a model which mixed some ^{56}Ni out to higher velocities would therefore help suppress the peak (see Branch et al. (1985); Jeffery et al. (1992)). The poor match is also likely in a part due to the approximate treatment of wavelength redistribution in our calculations (a constant $\epsilon = 0.05$ two level atom). In addition, the model suffers from an overly strong Fe III absorption just to the blue of the Si II 6150 feature.

The spectrum down the hole ($\theta = 0°$) is clearly very different than a normal SN Ia. We compare it to the peculiar SN 1991T, which it resembles in the following ways: (1) the Si II 6150 absorption is weak and has an unusually low velocity ($v \approx 10,000$ km s^{-1}); in addition, the Si II absorption at 4000 Åis absent. (2) The Ca II H&K feature is weak and split into two lines, explained as a blend of Ca II H&K and Si II λ3858 Nugent et al. (1997); in addition, the Ca II IR triplet absorption is absent. (3) In the iron blend near 5000 Å, the broad Fe II absorption is weak while the sharper Fe III blend is prominent (4) The UV portion of the spectrum (2500 Å$< \lambda <$ 3500 Å) is much brighter down the hole, due to the decreased line blocking.

There are also apparent differences between SN 1991T and the model, among them: (1) The S II "W-feature" near 5500 Åis weak but visible in the model, whereas no clear feature is seen in SN 1991T; (2) The model has too much emission in the Si II 6150 and Ca II IR triplet features. (3) The velocities of the Fe III lines are too low in the model, by about 2000 km s^{-1}. The Fe III lines are forming just at edge of the exposed iron/nickel core, so an explosion model that had a slightly larger ^{56}Ni zone than w7 would provide a better match SN 1991T. For now, though, the comparison of Figure 4 is meant only to demonstrate that the spectrum emanating from the hole could be characterized by so-called SN 1991T-like peculiarities. What connection, if any, the hole asymmetry may have to SN 1991T itself will be discussed further in the conclusion.

As can be seen in Figure 3, the spectrum changes continuously from peculiar to normal as the inclination is increased from zero. Some degree of peculiarity is seen for $\theta < \theta_H$, but the further the viewing angle is from 0°, the less intense the peculiarities. For a viewing angle of $\theta_H \approx 30°$, for instance, the depths of the Si II and Ca II features are about half that of the normal case and the iron blend near 5000 Å is dominated by Fe II rather than Fe III. One might rather compare the model from this viewing angle to SN 1999aa near maximum light, which was in many ways intermediate between SN 1991T and normal SN Ia.

We have also experimented with varying the density structure of the ejecta hole. As can be expected, increasing density in the hole tames the asymmetry and produces spectra with less intense peculiarities. Decreasing the hole opening angle weakness both the intensity and frequency of the peculiarities. If the hole density is increased past $f_H > 0.3$ or the opening angle reduced below $\theta_H < 20°$ the spectral peculiarities are minor from all lines of sight. In the models of Marietta et al. (2000), the hole opening angle is 40° in the low velocity layers, and $30° - 34°$ in the outer high-velocity layers, depending upon the nature of the companion star. The model used in Figures 3 and 4 ($\theta_H = 40°$ in all layers) thus represents the extreme end of what one might expect.

3.3. *Peak Magnitudes*

In the asymmetric ejecta-hole model, the observed luminosity depends upon line of sight. We plot the variation of the peak magnitude with inclination in Figure 5.

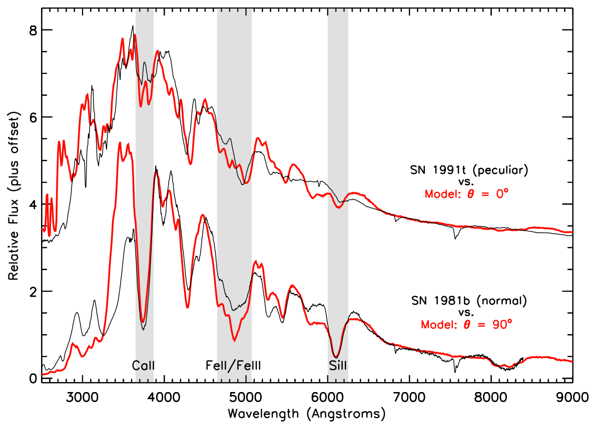

FIG. 4.— The maximum light spectra of the ejecta-hole model (red dotted lines) from two different inclinations are compared to two observed supernova (solid black lines). Bottom: the view from the side ($\theta = 90°$) compared to the normal SN Ia SN 1981B. Top: the view down the hole ($\theta = 0°$) compared to the peculiar SN Ia SN 1991T.

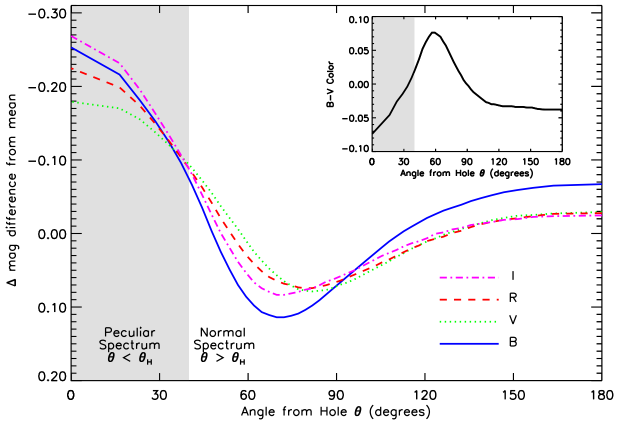

FIG. 5.— Variation with inclination of the B, V, R and I-band magnitudes of the ejecta-hole model near maximum light. The magnitudes are plotted relative to the mean magnitude averaged over all inclinations. The inset shows the variation of the B-V color.

When viewed near or down the hole ($\theta < \theta_H$) the supernova is brighter than average by 0.1-0.3 mag in B. This is because photons more readily escape out the hole due to the lower opacities. It is widely believed that observed SN 1991T-like supernova are in general overluminous, although the degree and regularity of this overluminosity can be questioned (Saha et al. 2001). While Figure 5 suggests a similar correlation, keep in mind that this line of sight of variation is only one possible source of luminosity diversity in SN Ia, and apparently a sub-dominant one at that. The luminosity will depend predominately on the amount of ^{56}Ni synthesized in the explosion, which is also presumed to vary from case to case. If a SN Ia has a very small ^{56}Ni mass, for example, then although the view down the hole is the brightest of all possible viewing angles, the supernova would still appear underluminous

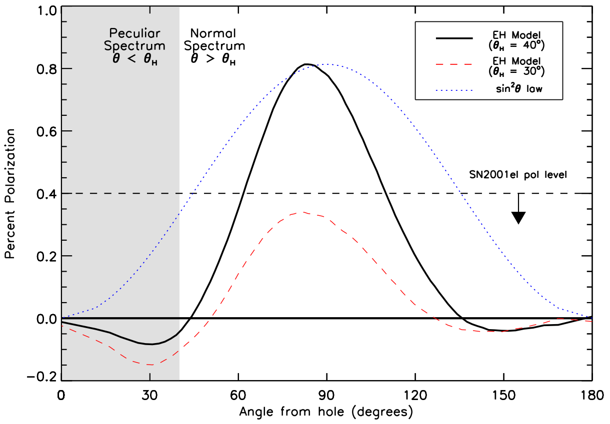

FIG. 6.— Continuum polarization of the ejecta-hole model near maximum light as a function of inclination. The solid black line is the model used throughout the paper, while the red dashed line is a model where the hole opening angle has been reduced to 30°. We also overplot for comparison $\sin^2\theta$ (multiplied by 0.8%), which is the inclination dependence of an optically thin scattering envelope.

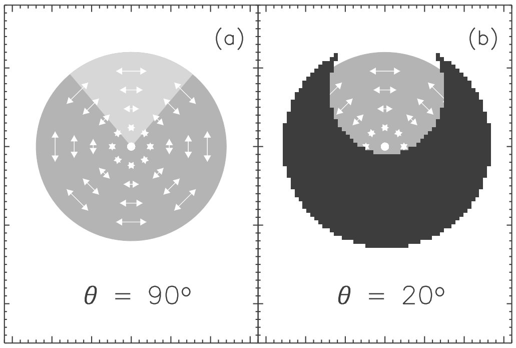

FIG. 7.— Schematic diagram which helps explain the polarization in the ejecta hole model. Left: when viewed from the side ($\theta \approx 90°$) the top of the atmosphere is lacking a wedge of scatterers. The vertically polarized flux thus exceeds the horizontal and the continuum polarization is positive. Right: When viewed just off the hole axis ($\theta \approx 20°$), the line opacity on the planar surface corresponding to a certain line of sight blueshift (shown in black) only partially covers the photosphere. Because of the hole, horizontally polarized flux from the top of the atmosphere is relatively unobscured by the line and will cause the negatively polarized line peaks.

compared to a SN Ia with normal ^{56}Ni production.

For those lines of sight where the spectrum looks normal ($\theta > \theta_H$) the ejecta-hole asymmetry still causes some dispersion in peak magnitude. For example, the supernova is dimmer when viewed from the side ($\theta = 90°$) then from the back ($\theta = 180°$), because when viewed from the side the supernova is lacking a "wedge" of emitting material (see Figure 7a). The total dispersion about the mean in the ejecta hole model is V and R is 0.1 mag, and somewhat larger in B (0.2 mag) as a result of the B-band's greater sensitivity to line opacity. One must keep in mind that the computed magnitudes can be sensitive to the details of the model. Decreasing the hole size to $\theta_H = 30°$ decreases the B-band dispersion to $\sim$0.1 mag. Because of the importance of line opacity in the spectrum formation, the magnitudes can also be sensitive to the particular elemental composition structure used.

The observed dispersion in SN Ia peak magnitudes is around 0.3 mag in the B-band, and the brightness is found to correlate with the width of the light curve (Phillips et al. 1999). This dispersion is believed to be largely the result of varying amounts of ^{56}Ni synthesized in the explosion. After correction for the width-luminosity relation and dust extinction (using the B-V color), the observed dispersion is reduced to $\sim 0.15 - 0.2$ mag Hamuy et al. (1996). Some of this residual dispersion may be due to an asymmetry of some sort; in fact Figure 5 suggests that in the particular case of an ejecta-hole asymmetry, the residual might be largely or entirely due to the asymmetry. Note, however, that in the ejecta-hole model the B-V color roughly correlates with peak magnitude – thus correcting for dust extinction with a B-V color will tend to correct for the asymmetry also.

3.4. *Continuum Polarization*

The polarization is the most direct indication of asymmetry in the ejecta. Because a spherically symmetric atmosphere has no preferred direction, the polarization integrated over the projected supernova surface must cancel. In an axially-symmetric geometry like the ejecta-hole model, the net polarization can be non-zero and will align either parallel or perpendicular to the axis of symmetry. We use the convention that positive (negative) polarization designates a polarization oriented parallel (perpendicular) to the axis of symmetry. SN 2001el had a well-defined polarization angle over most of the spectral features, which indicates that the bulk of the ejecta obeyed a near axial symmetry (in addition, SN 2001el showed an unusual high velocity Ca II IR triple feature with a distinct polarization angle, corresponding to a detached "clump" of material that deviated from the dominant axis of symmetry(Kasen et al. 2003)).

Light becomes polarized in supernova atmospheres due to electron scattering; other sources of opacity, such as bound-bound line transitions, are usually considered to be depolarizing. We define the continuum polarization as the polarization computed using only electron scattering opacity – this is most closely realized in the red end of a supernova spectrum (say near 7000 Å), where there is not much line opacity. However this may not be the maximum polarization level in the spectrum, as the line opacity may partially obscure the underlying photosphere and lead to a less effective cancellation of the polarization in the line features (see § 3.5 and (Kasen et al. 2003)).

Figure 6 shows the ejecta-hole model continuum polarization as a function of inclination. When viewed directly down the hole ($\theta = 0°$) the projection of the supernova atmosphere is circularly symmetric and the polarization cancels. As the line of sight is inclined, the polarization increases, reaching a maximum when the supernova is viewed nearly side-on ($\theta \approx 90°$). The origin of the non-zero polarization is clear from Figure 7a. At inclinations near 90°, the hole removes a "wedge" of scatterers from the top of the atmosphere, which decreases the horizontally polarized flux coming from this region. The vertically polarized flux thus exceeds the horizontally polarized flux; the net polarization is non-zero and aligned with the symmetry axis of the system (positive according to our convention).

To determine the level of intrinsic continuum polarization in observed supernova, one must wrestle with the issue of subtracting the interstellar polarization (Howell et al. 2001; Leonard et al. 2000). Once this is done, the observed levels are found to be rather small: the polarization of SN 2001el was ~0.4% in the premaximum observations which decreased to $\sim 0.3\%$ near maximum light. The polarization of the subluminous SN 1999by near maximum light was $\sim$ 0.7%. For several other SNe Ia, no polarization signal was detected, but upper limits of 0.3-0.5% can be derived (Wang et al. 1996a,b). In the ejecta-hole model, the continuum polarization can be as large as 0.8% and the polarization at the line features can be even larger (see next section). The hole asymmetry therefore produces polarization levels in the right range, though perhaps generally too high compared to the observations. The level in the model, however, is rather sensitive to the size and density of the ejecta hole. To demonstrate this we have over-plotted the continuum polarization of a model with a opening angle $\theta_H = 30°$. This tames the asymmetry and decrease the continuum polarization by more than a factor of two. If the hole size is decreased further to $\theta_H < 20°$, the continuum polarization level is uninterestingly small ($\lesssim 0.1\%$) from all inclinations. Thus the exact polarization level will depend upon the hole structure, which depends upon the details of the progenitor system and hydrodynamics. In general, the more extreme the asymmetry of the hole (i.e. the larger and more evacuated it is) the higher the average polarization level. A larger sample of SN Ia spectropolarimetry could therefore put constraints on the size of a putative hole.

The dependence of the ejecta-hole polarization on inclination can be compared to the $\sin^2\theta$ law appropriate for optically thin envelopes (Brown & McLean 1977). The two are quite different because of multiple scattering effects in the optically thick supernova envelope. One correlation to keep in mind is that the continuum polarization is always relatively small ($\lesssim 0.1\%$) for views near the hole where the spectrum looks peculiar. For views away from the hole, the continuum polarization may be either small or large. However the continuum polarization is not the whole story and as we see in the next section, the polarization over the line features can be substantial even for $\theta < \theta_H$.

3.5. *Polarization Spectrum*

The continuum polarization level actually provides very little information as to the nature of the ejecta asymmetry, as very different configurations can give the same numerical value. Line features in the polarization spectrum, on the other hand, contain more potential information about the geometry. We find that the ejecta-hole model has spectropolarimetric signatures that distinguish it from, for example, an ellipsoidal geometry.

The polarization spectrum in the ellipsoidal geometry has been studied in detail (Jeffrey 1989; Höflich et al. 1996). In ellipsoidal models, the polarization level generally increases from blue to red due to the greater amount of depolarizing line opacity in the blue. Individual lines create "inverted P-Cygni" profiles in the polarization spectrum, i.e. a blueshifted polarization peak with a redshifted depolarization trough. The blueshifted peak is a result of the line opacity preferentially blocking the lowly polarized central photospheric light, while the redshifted trough is the result of unpolarized line emission light diluting the continuum polarization. The polarized line profiles look fairly similar from all inclinations.

The line polarization profile in the ejecta-hole model shows an interesting variation with inclination (Fig-

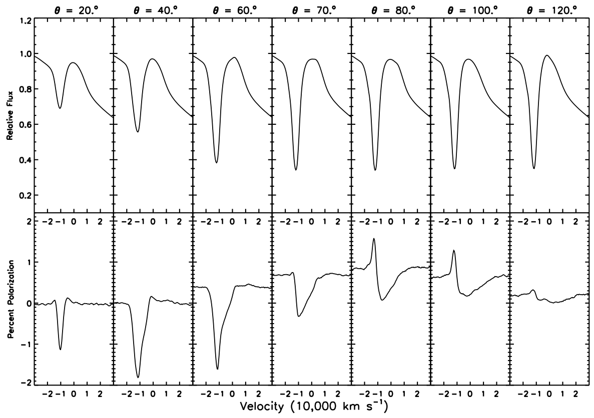

FIG. 8.— Flux and polarization profiles of a single unblended line in the ejecta-hole geometry from various lines of sight. The polarization feature is a peak for low inclinations and an inverted P-Cygni for views near the side ($\theta \approx 90°$).

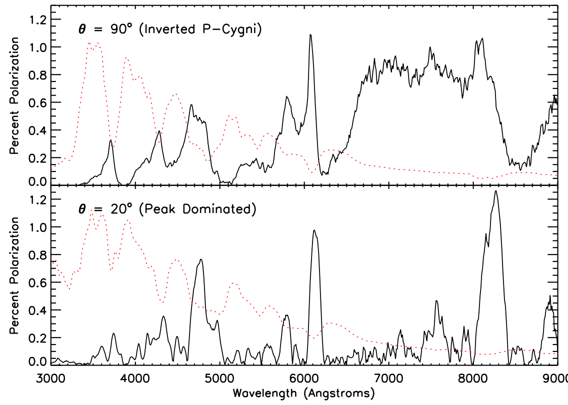

FIG. 9.— Polarization spectrum of the ejecta-hole model near maximum light for two lines of sight. We plot the absolute value of the polarization (solid lines), and for reference overlay the flux spectrum (dotted lines). The small scale wiggles in the polarization spectrum are Monte Carlo noise, which increases to the red due to the lower fluxes. Top: for views away from the hole (here $\theta = 90°$) the spectrum resembles that of an ellipsoidal geometry with "inverted P-Cygni" line profiles. Bottom: for views near the hole (here $\theta = 20°$), the spectrum is "peak-dominated" with a low continuum polarization but substantial line peaks.

ure 8). For views far enough away from the hole ($\theta \gtrsim 80°$), the profile is an inverted P-Cygni just as in an ellipsoidal model and for essentially the same reason. For views closer to the hole, however, the blueshifted line absorption gives rise to a large polarization peak. This peak is negative, where recall the negative sign indicates that the polarization direction is perpendicular to the symmetry axis of the system. Figure 7b helps explain the origin of the peak. From viewing angles near the hole axis, the projected electron scattering medium is fairly symmetric and the continuum polarization integrated over the ejecta surface nearly cancels. The line opacity, however, only partially obscures the underlying light. Because of the hole, horizontally polarized flux from the top of the atmosphere is relatively unobscured by the line, whereas the vertically polarized light from the sides of the atmosphere is effectively screened. The polarization over the line therefore does not cancel but will be large and oriented perpendicular to the axis of symmetry (negative according to our convention). Note that if the hole opening angle is narrowed to $\theta = 30°$, the line is even more effective in screening off all but the horizontally polarized light. The line polarization peak is therefore *larger.* Thus while the continuum polarization decreases with decreasing hole size, the line polarization from certain viewing angles will be relatively large ($\sim 1.0\%$) regardless of how big the hole is.

Figure 9 shows the entire ejecta-hole polarization spectrum from two lines of sight. For a view near the hole ($\theta = 20°$) the spectrum is "line peak-dominated" – the continuum polarization is rather low, but large polarization peaks are associated with the blueshifted line absorption features (in particular the Si II 6150 feature and the Ca II IR triplet). This spectrum is qualitatively different than what is expected in an ellipsoidal geometry. For views away from the hole ($\theta = 90°$), on the other hand, the polarization spectrum would be very hard to distinguish from the ellipsoidal case. The level of polarization rises from blue to red and the line features due to Si II 6150 feature and Ca II IR triplet have the "inverted P-Cygni" profile. The shape of the polarization spectrum from these angles resembles SN 2001el, although the polarization level is too high unless $\theta \gtrsim 110°$, or the hole opening angle is reduced.

To discriminate between different geometries, a larger sample of polarization spectra is needed. If the asymmetry in SN Ia is an ejecta-hole we would expect to see something like a line peak dominated polarization spectrum about 25% of the time. Such a polarization spectrum has not be observed as yet, but the number of spectropolarimetric observations is still relatively small. In addition, if the level of interstellar polarization is unknown, then the zeropoint of the intrinsic supernova polarization is unknown and it will be unclear whether features in the polarization spectrum are peaks or troughs. Therefore multi-epoch spectropolarimetric observations may be necessary to help pin down the ISP. Of course, observing a line peak dominated polarization spectrum would not necessarily uniquely imply an ejecta hole, as large line peaks could potentially occur in other geometries, for example an atmosphere with large scale clumpiness in composition.

4. CONCLUSION

Despite the seemingly extreme nature of an ejecta-hole asymmetry, we find that the geometry is actually consistent with what is currently known about SNe Ia, at least for the observables we have calculated. The dispersion in peak magnitudes induced by the hole is sufficiently small, and the level of polarization in the range detected by spectropolarimetric observations. The spectrum of the supernova looks peculiar when viewed near the hole, but this peculiarity may fit in with the spectral diversity already known to exist in SN Ia. In addition the polarization spectrum from some lines of sight is a qualitative match to that of SN 2001el.

An ejecta-hole asymmetry could therefore be one source of diversity in SN Ia, but of course not the only one. The primary source of diversity in SN Ia is thought to be due to variations in the amount of ^{56}Ni produced in the explosion. Because SN Ia are powered by the radioactive decay of ^{56}Ni and its daughter ^{56}Co , different ^{56}Ni production can explain the variety in SN Ia peak magnitudes. The greater ^{56}Ni masses may lead to higher atmospheric temperatures and higher effective opacities, which may explain why brighter SN Ia have broader light curves (Hoflich et al. 1995; Pinto & Eastman 2000a). It has often been thought that the spectroscopic diversity of SN Ia fits into the same one-parameter ^{56}Ni sequence (Nugent et al. 1995). In this picture SN 1991T-like supernova occupy the overluminous end of the sequence, where the larger ^{56}Ni mass leads to higher envelope temperatures and a higher ionization fraction. This can explain the peculiar spectral appearance (Mazzali et al. 1995; Jeffery et al. 1992). As the models in this paper show, if an ejecta-hole asymmetry exists, there is a physically very different route to the same sort of spectral peculiarities. In the ejecta-hole model, the spectrum shows some level of peculiarity for $\theta \lesssim \theta_H$ or about 12% of the time, although the peculiarities will only be very intense for views more directly down the hole ($\theta \lesssim \theta_H/2$ or $\sim 3\%$ of the time). The observed rate of SN 1991T-like supernova is $\sim 3-5\%$ in the samples of Branch (2001) and Li et al. (2001b); the rate of SN 1991T/SN 1999aa-like supernova is $\sim 20\% \pm 7\%$ in the Li et al. (2001b) sample. Therefore it is possible that a substantial percentage of these peculiar supernovae could be the result of an ejecta-hole asymmetry.

In this paper we have chosen to compare the spectra emanating from the hole with SN 1991T only because it is the well-known prototype of a certain kind of spectral peculiarity. Whether SN 1991T itself was an example of merely looking down an ejecta hole is debatable. Initial estimates suggested that SN 1991T was as much as 0.7-0.8 magnitudes brighter in B than normal, which is too much to be explained by the asymmetry alone (Fisher et al. 1999). More recent Cepheid measurements of the distance to the host galaxy, however, give a more moderate overluminosity of 0.3 mag, although a value as high 0.6 mag cannot be ruled out (Saha et al. 2001) (the large uncertainty is due to uncertainty in the substantial dust extinction). This lower value for the brightness of SN 1991T calls into question whether the peculiar spectral appearance can still be explained alone by high envelope temperatures due to a larger ^{56}Ni mass.

SN 1991T also had an unusually broad light curve ($\Delta M_{15} = 0.95 \pm 0.05$; Phillips et al. (1999)), which is often taken as an indication of a large ^{56}Ni mass. Because we have not yet computed time-dependent models, we do not know exactly what effect the ejecta hole asymmetry would have on the light curve. We know that there will be some line of sight variation, because the directional diffusion time and distribution of gamma-ray deposited energy will vary with time, as will the line of sight dependence of the colors. In any case, although the prototype SN 1991T did have a broad light curve, it can be questioned whether this correlation holds in general. SN 1997br, a SN 1991T-like supernova, did have a rather broad light curve (Δ M_{15}= 1.00 $\pm$ 0.15; Li et al. (1999)). Several other SNe Ia, however, have similar or broader light curves, and yet the spectrum is apparently normal. At least eight such supernova with $\Delta M_{15} < 1.0$ are listed in Phillips et al. (1999), for example SN 1992bc (Δ M_{15}= 0.87 $\pm$ 0.05) and SN 1994ae (Δ M_{15}= 0.86 $\pm$ 0.05). SN 2001ay also had a normal spectrum but an exceptionally broad light curve (Δ M_{15}= 0.6-0.7; Phillips et al. (2003)). Among the SN 1991T-like supernovae, there also appears to be diversity in the light curves. SN 2002cx, which resembled SN 1991T spectroscopically in some ways (to be discussed shortly), had a B-band light curve of normal width ($\Delta M_{15} = 1.30 \pm 0.09$; Li et al. (2003)). In another SN 1991T-like supernova, SN 2000cx, the B-band light curve was lopsided (Li et al. 2001a). SN 2000cx brightened much faster than SN 1991T (resembling the rise of the normal SN 1994D) but the decline was slow (Δ M_{15}= 0.93 $\pm$ 0.04). The examples make it clear that any connection between light curve width and SN 1991T-like spectral peculiarities remains vague.

The nebular spectra of SN 1991T may also suggest a large ^{56}Ni production. In the late time spectra, the iron emission lines of SN 1991T have larger velocity widths than in most SN Ia(Mazzali et al. 1998). Assuming the late time ionization/excitation conditions are similar in all SN Ia, this implies that the Nickel/Iron core in SN 1991T is larger than normal. Confusing this conclusion, however, is the fact pointed out by Hatano et al. (2002) that the Si II velocities in the post maximum spectra are among the *lowest* of all SNe Ia. If SN 1991T really did have a large inner ^{56}Ni zone, one might expect that the zone of silicon and other intermediate mass elements would occur at especially high velocities (as for instance in the delayed detonation models of e.g. Höflich et al. (2002)). To account for the low Si II velocities, some have invoked a late-detonation model for SN 1991T, which produces a layer of intermediate mass elements sandwiched between two nickel zones (Yamaoka et al. 1992; Ruiz-Lapuente et al. 1992). Of course a lower Si II velocity is also naturally expected if one is looking down an ejecta hole.

It is likely that SN 1991T did have a relatively large ^{56}Ni mass, rather than (or perhaps in addition to) being viewed down the ejecta hole. However among other supernova with SN 1991T-like peculiarities there is a good deal of diversity, and the large ^{56}Ni mass explanation will not apply in all cases. The most obvious case in point is SN 2002cx (Li et al. 2003). The spectrum of SN 2002cx resembled SN 1991T in that Si II, S II, and Ca II lines were weak, while Fe III was prominent, but the supernova was *underluminous* by ~ 2 mag. The velocity of the absorption features was also unusually low ($v \approx 7.000$ km s^{-1}). The singularity of the supernova lead Li et al. (2003) to consider alternative progenitor systems, although they concluded that no existing theoretical model could explain all the peculiarities. On the other hand, there is also the possibility that we are seeing multiple channels of diversity operating at once – one scenario to entertain now is that we are looking down the ejecta hole of a "weak" supernova that produced a small mass of ^{56}Ni . Such underluminous objects like SN 1991bg typically have relatively low absorption velocities (Turatto et al. 1996; Mazzali et al. 1997; Hatano et al. 2002) which be further reduced by looking down the hole. Despite the low luminosity, the spectrum might still appear hot and iron dominated if one is peering into the deeper layers, and (eventually) into the iron core. Of course, the chance of seeing two distinct sources of diversity operating at once would be, like SN 2002cx, a very rare occurrence.

Whatever the final explanation for SN 2002cx, its singularity highlights the fact that the diversity of SNe Ia is more complicated than a one-parameter sequence based upon ^{56}Ni . One can imagine many sources of variation contributing, including: different amounts and distributions of high-velocity material, different sizes and inclinations of an ejecta hole (or other) asymmetry, various explosion processes (e.g. pure deflagration, deflagration-to-detonation, late-detonation) and even the possibility of completely different progenitor channels (e.g. a double-degenerate scenario). With so much going on at once, interpreting the observations becomes a daunting task, but in some sense the identification of multiple channels of diversity is welcome, considering that observations continue to turn up unusual SNe Ia.

The results of this paper suggest a few observational signatures of the ejecta-hole geometry. First the continuum polarization should be low for views near the hole, where the spectrum looks peculiar. However because of the partial obscuration effect, the line polarization can be substantial from these inclinations – i.e the polarization spectrum should look line peak-dominated. For views from the side, the higher continuum polarization should be correlated with a slightly dimmer supernova with normal spectral features and inverted P-Cygni line polarization features. Another possible signature of the ejecta hole is "lopsided" P-Cygni flux profiles – the view down the hole weakens only the absorption, not the emission feature, so one could look for a weak (or absent) absorption associated with noticeable emission. The easiest place to look would be in the Si II 6150 and the Ca II IR triplet features. Unfortunately the relative strength of absorption to emission depends also on the line source function, which is determined by the detailed excitation conditions in the atmosphere. In general, because we recognize that an ejecta-hole asymmetry is only one of several possible sources of diversity in SN Ia, it will be difficult to isolate the geometrical effects from the other variations that may be operating. The only hope is to collect a large sample of supernova with well observed light curves, spectra and polarization, so that one might try to pull out the different trends.

In our calculations we have used a parameterized hole (half opening angle 40°) in order to explore the essential observable consequences of the geometry. The next step is to address the same questions using specific hydrodynamical models representing a wide variety of initial configurations. Potentially the details of the progenitor system could affect the size and shape of the hole. Marietta et al. (2000) compute interactions using main sequence, subgiant and red giant companions and note that the variation in the hole asymmetry is not large. This is because in all cases the companion star is near enough to have undergone Roche lobe overflow and always occupies a similar solid angle (the red giant is farther away but physically larger than a main sequence companion which is smaller but much closer). However if the ratio of companion radius to separation distance is decreased, the size of the hole also decreases. A larger sample of spectropolarimetric observations will help determine if SN Ia really do have an ejecta-hole geometry, and could constrain the hole opening angle if one exists. While a hole smaller than $\theta < 20^\circ$ has only minor effects on the spectrum, luminosity and continuum polarization, it will still create substantial line peaks in the polarization spectrum when seen from some viewing angles. If signatures of the hole are not seen in future spectropolarimetric observations then, this would have interesting consequences for the progenitors of SN Ia, or the hydrodynamics of the ejecta/companion interaction.

Finally, we mention that an asymmetry like an ejecta hole could have consequences on the use of SN Ia as standard candles for cosmology. The asymmetry causes a dispersion in peak magnitude. If the asymmetry is identical in all SNe Ia, this dispersion simply behaves like a statistical error and by observing enough objects one accurately determines the average peak magnitude. However if the nature, degree, or frequency of the asymmetry evolves with redshift (say because of evolving progenitor populations) the average peak magnitude of SN Ia becomes a function of redshift. The resulting systematic effect would be relatively small, but may need to be considered in the next generation of precision supernova cosmology experiments.

REFERENCES

Branch, D. 1987, ApJ, 316, L81
—. 2001, PASP, 113, 169
Branch, D., Doggett, J. B., Nomoto, K., & Thielemann, F.-K. 1985, ApJ, 294, 619
Branch, D., Fisher, A., & Nugent, P. 1993, AJ, 106, 2383
Branch, D., Livio, M., Yungelson, L. R., Boffi, F. R., & Baron, E. 1995, PASP, 107, 1019
Branch, D. et al. 2003, ApJ, in preperation
Brown, J. C. & McLean, I. S. 1977, A&A, 57, 141+
Code, A. D. & Whitney, B. A. 1995, ApJ, 441, 400
Filippenko, A. V., Richmond, M. W., Branch, D., Gaskell, M., Herbst, W., Ford, C. H., Treffers, R. R., Matheson, T., Ho, L. C., Dey, A., Sargent, W. L. W., Small, T. A., & van Breugel, W. J. M. 1992a, AJ, 104, 1543
Filippenko, A. V., Richmond, M. W., Matheson, T., Shields, J. C., Burbidge, E. M., Cohen, R. D., Dickinson, M., Malkan, M. A., Nelson, B., Pietz, J., Schlegel, D., Schmeer, P., Spinrad, H., Steidel, C. C., Tran, H. D., & Wren, W. 1992b, ApJ, 384, L15
Fisher, A., Branch, D., Hatano, K., & Baron, E. 1999, MNRAS, 304, 67
Fryxell, B. A. & Arnett, W. D. 1981, ApJ, 243, 994
Höflich, P., Gerardy, C. L., Fesen, R. A., & Sakai, S. 2002, ApJ, 568, 791
Hamuy, D. et al. 2003, Nature, accepted; astro-ph/0306270
Hamuy, M., Phillips, M. M., Suntzeff, N. B., Schommer, R. A., Maza, J., & Aviles, R. 1996, AJ, 112, 2391
Hatano, K., Branch, D., Fisher, A., Baron, E., & Filippenko, A. V. 1999, ApJ, 525, 881
Hatano, K., Branch, D., Qiu, Y. L., Baron, E., Thielemann, F.-K., & Fisher, A. 2002, New Astronomy, 7, 441
Hoflich, P., Khokhlov, A. M., & Wheeler, J. C. 1995, ApJ, 444, 831
Höflich, P., Wheeler, J. C., Hines, D. C., & Trammell, S. R. 1996, ApJ, 459, 307+
Howell, D. A., Höflich, P., Wang, L., & Wheeler, J. C. 2001, ApJ, 556, 302
Jeffery, D. J., Leibundgut, B., Kirshner, R. P., Benetti, S., Branch, D., & Sonneborn, G. 1992, ApJ, 397, 304
Jeffrey, D. J. 1989, ApJS, 71, 951
—. 1991, ApJ, 375, 264
Kasen, D., Nugent, P., Wang, L., Howell, D. A., Wheeler, J. C., Höflich, P., Baade, D., Baron, E., & Hauschildt, P. H. 2003, ApJ, 593, 788
Kasen, D. e. a. 2003, in preperation
Lentz, E. J., Baron, E., Branch, D., & Hauschildt, P. H. 2001, ApJ, 557, 266
Leonard, D. C., Filippenko, A. V., Barth, A. J., & Matheson, T. 2000, ApJ, 536, 239
Li, W., Filippenko, A. V., Chornock, R., Berger, E., Berlind, P., Calkins, M. L., Challis, P., Fassnacht, C., Jha, S., Kirshner, R. P., Matheson, T., Sargent, W. L. W., Simcoe, R. A., Smith, G. H., & Squires, G. 2003, PASP, 115, 453
Li, W., Filippenko, A. V., Gates, E., Chornock, R., Gal-Yam, A., Ofek, E. O., Leonard, D. C., Modjaz, M., Rich, R. M., Riess, A. G., & Treffers, R. R. 2001a, PASP, 113, 1178
Li, W., Filippenko, A. V., Treffers, R. R., Riess, A. G., Hu, J., & Qiu, Y. 2001b, ApJ, 546, 734
Li, W. D., Qiu, Y. L., Qiao, Q. Y., Zhu, X. H., Hu, J. Y., Richmond, M. W., Filippenko, A. V., Treffers, R. R., Peng, C. Y., & Leonard, D. C. 1999, AJ, 117, 2709
Livne, E., Tuchman, Y., & Wheeler, J. C. 1992, ApJ, 399, 665
Lucy, L. B. 1999, A&A, 344, 282
Marietta, E., Burrows, A., & Fryxell, B. 2000, ApJS, 128, 615
Mazzali, P. A., Cappellaro, E., Danziger, I. J., Turatto, M., & Benetti, S. 1998, ApJ, 499, L49+
Mazzali, P. A., Chugai, N., Turatto, M., Lucy, L. B., Danziger, I. J., Cappellaro, E., della Valle, M., & Benetti, S. 1997, MNRAS, 284, 151
Mazzali, P. A., Danziger, I. J., & Turatto, M. 1995, A&A, 297, 509
Mazzali, P. A. & Lucy, L. B. 1993, A&A, 279, 447
Nomoto, K., Thielemann, F., & Yokoi, K. 1984, ApJ, 286, 644
Nugent, P., Baron, E., Branch, D., Fisher, A., & Hauschildt, P. H. 1997, ApJ, 485, 812
Nugent, P., Phillips, M., Baron, E., Branch, D., & Hauschildt, P. 1995, ApJ, 455, L147+
Phillips, M. M., Krisciunas, K., Suntzeff, N. B., Roth, M., Germany, L., Candia, P., Gonzalez, S., Hamuy, M., Freedman, W. L., Persson, S. E., Nugent, P. E., Aldering, G., & Conley, A. 2003, in From Twilight to Highlight: The Physics of Supernovae. Proceedings of the ESO/MPA/MPE Workshop held in Garching, Germany, 29-31 July 2002, p. 193., 193–+
Phillips, M. M., Lira, P., Suntzeff, N. B., Schommer, R. A., Hamuy, M., & Maza, J. 1999, AJ, 118, 1766
Phillips, M. M., Wells, L. A., Suntzeff, N. B., Hamuy, M., Leibundgut, B., Kirshner, R. P., & Foltz, C. B. 1992, AJ, 103, 1632
Pinto, P. A. & Eastman, R. G. 2000a, ApJ, 530, 744
—. 2000b, ApJ, 530, 757
Ruiz-Lapuente, P., Cappellaro, E., Turatto, M., Gouiffes, C., Danziger, I. J., della Valle, M., & Lucy, L. B. 1992, ApJ, 387, L33
Saha, A., Sandage, A., Thim, F., Labhardt, L., Tammann, G. A., Christensen, J., Panagia, N., & Macchetto, F. D. 2001, ApJ, 551, 973
Thomas, R. C., Kasen, D., Branch, D., & Baron, E. 2002, ApJ, 567, 1037
Thomas, R. C. et al. 2003, ApJ, submitted; astro-ph/0302260
Turatto, M., Benetti, S., Cappellaro, E., Danziger, I. J., della Valle, M., Gouiffes, C., Mazzali, P. A., & Patat, F. 1996, MNRAS, 283, 1
Wang, L., Wheeler, J. C., Li, Z., & Clocchiatti, A. 1996a, ApJ, 467, 435+
—. 1996b, ApJ, 467, 435
Wang, L. et al. 2003, ApJ, in press

Wheeler, J. C., Lecar, M., & McKee, C. F. 1975, ApJ, 200, 145
Yamaoka, H., Nomoto, K., Shigeyama, T., & Thielemann, F. 1992, ApJ, 393, L55